

# Sharp and asymmetric transmission response in metal-dielectric-metal plasmonic waveguides containing Kerr nonlinear media

Zhi-Jian Zhong, Yi Xu, Sheng Lan, Qiao-Feng Dai, and Li-Jun Wu\*

Laboratory of Photonic Information Technology, School for Information and Optoelectronic Science and Engineering, South China Normal University, Guangzhou 510006, P.R. China

\*ljwu@scnu.edu.cn

**Abstract:** Based on the excitation of surface plasmon polaritons (SPPs), we analytically and numerically investigate the transmission response in metal-dielectric-metal (MDM) plasmonic waveguides with a side coupled nanocavity (SCNC). By filling the nanocavity with a Kerr nonlinear medium, the position of the resonant dip in the transmission spectrum can be tuned by the incident light intensity. The oscillation of a Fabry-Perot nanocavity formed by incorporating a finite length of the same Kerr nonlinear media into the MDM waveguide acts as a background for the transmission response of the system and induces a sharp and asymmetric response line shape. As a result, the wavelength shift required for the plasmonic device to be switched from the maximum to the minimum transmission can be reduced by half in a structure less than 400 nm long. Such an effect may be potentially applied to constructing SPP-based all-optical switching with low power threshold at nanoscale.

©2009 Optical Society of America

**OCIS codes:** (240.6680) Surface Plasmons; (260.3910) Optics of Metal; (130.3120) Integrated optics devices; (230.7370) Waveguide.

---

## References and links

1. H. M. Gibbs, *Optical bistability: Controlling Light with Light*, (Academic, New York, 1985).
2. X. Hu, P. Jiang, C. Ding, H. Yang, and Q. Gong, "Picosecond and low-power all-optical switching based on an organic photonic-bandgap microcavity," *Nat. Photonics* **2**(3), 185–189 (2008).
3. X. S. Lin, J. H. Yan, L. J. Wu, and S. Lan, "High transmission contrast for single resonator based all-optical diodes with pump-assisting," *Opt. Express* **16**(25), 20949–20954 (2008).
4. Y. Shen, and G. P. Wang, "Optical bistability in metal gap waveguide nanocavities," *Opt. Express* **16**(12), 8421–8426 (2008).
5. B. Wang, and G. P. Wang, "Plasmon bragg reflectors and nanocavities on flat metallic surfaces," *Appl. Phys. Lett.* **87**(1), 013107 (2005).
6. E. Ozbay, "Plasmonics: merging photonics and electronics at nanoscale dimensions," *Science* **311**(5758), 189–193 (2006).
7. C. Min, P. Wang, C. Chen, Y. Deng, Y. Lu, H. Ming, T. Ning, Y. Zhou, and G. Yang, "All-optical switching in subwavelength metallic grating structure containing nonlinear optical materials," *Opt. Lett.* **33**(8), 869–871 (2008).
8. G. A. Wurtz, R. Pollard, and A. V. Zayats, "Optical bistability in nonlinear surface-plasmon polaritonic crystals," *Phys. Rev. Lett.* **97**(5), 057402 (2006).
9. E. N. Economou, "Surface plasmons in thin films," *Phys. Rev.* **182**(2), 539–554 (1969).
10. J. A. Dionne, L. A. Sweatlock, H. A. Atwater, and A. Polman, "Planar metal plasmon waveguides: frequency-dependent dispersion, propagation, localization, and loss beyond the free electron model," *Phys. Rev. B* **72**(7), 075405 (2005).
11. A. Hosseini, and Y. Massoud, "Nanoscale surface plasmon based resonator using rectangular geometry," *Appl. Phys. Lett.* **90**(18), 181102 (2007).
12. S. Xiao, L. Liu, and M. Qiu, "Resonator channel drop filters in a plasmon-polaritons metal," *Opt. Express* **14**(7), 2932–2937 (2006).
13. X. S. Lin, and X. G. Huang, "Tooth-shaped plasmonic waveguide filters with nanometric sizes," *Opt. Lett.* **33**(23), 2874–2876 (2008).
14. Y. Matsuzaki, T. Okamoto, M. Haraguchi, M. Fukui, and M. Nakagaki, "Characteristics of gap plasmon waveguide with stub structures," *Opt. Express* **16**(21), 16314–16325 (2008).

15. C. Min, and G. Veronis, "Absorption switches in metal-dielectric-metal plasmonic waveguides," *Opt. Express* **17**(13), 10757–10766 (2009).
  16. Z. Yu, G. Veronis, S. Fan, and M. L. Brongersma, "Gain-induced switching in metal-dielectric-metal plasmonic waveguides," *Appl. Phys. Lett.* **92**(4), 041117 (2008).
  17. E. D. Palik, *Handbook of Optical Constants of Solids*, (Academic, Boston, 1985).
  18. A. Taflov, and S. C. Hagness, *Computational Electrodynamics* (Artech House, Norwood, MA, 2000), In this paper, a commercial software developed by Rsoft Design Group (<http://www.rsoftdesign.com>) is used for nonlinear FDTD simulation.
  19. R. W. Boyd, *Nonlinear Optics*, (Academic, New York, 1992).
  20. H. A. Haus, and Y. Lai, "Theory of Cascaded Quarter Wave Shifted Distributed Feedback Resonators," *IEEE J. Quantum Electron.* **28**(1), 205–213 (1992).
  21. H. F. Shi, C. T. Wang, C. L. Du, X. G. Luo, X. C. Dong, and H. T. Gao, "Beam manipulating by metallic nano-slits with variant widths," *Opt. Express* **13**(18), 6815–6820 (2005).
  22. S. Fan, "Sharp asymmetric line shapes in side-coupled waveguide-cavity systems," *Appl. Phys. Lett.* **80**(6), 908 (2002).
  23. Y. Xu, Y. Li, R. K. Lee, and A. Yariv, "Scattering-theory analysis of waveguide-resonator coupling," *Phys. Rev. E Stat. Phys. Plasmas Fluids Relat. Interdiscip. Topics* **62**(5 5 Pt B), 7389–7404 (2000).
  24. H. A. Haus, *Wave and Fields in Optoelectronics*, (Prentice-Hall, Englewood Cliffs, NJ, 1984).
- 

## 1. Introduction

Controlling light with light is essential in all-optical signal processing in integrated photonic circuits and its application in optical communications networks [1,2]. All optical devices based on various types of optical nonlinearities have been proposed during past years. The main drawbacks of most of such devices, however, are the limitation on their minimum size required to provide a sufficient light pass to achieve enough nonlinear response, and relatively high operating light intensity. To overcome these drawbacks, nonlinear optical devices based on photonic crystal defects have been proposed by utilizing the confinement of electromagnetic field at the photonic defect location to enhance nonlinear effects [2,3]. Due to the effect of enhancing the local optical field intensity, surface plasmon polaritons (SPPs) provide another useful platform to realize strong nonlinear effects in all-optical devices [4–8]. For example, optical bistability has been realized in metal-dielectric nanocavities based on Fabry-Perot (F-P) effect [4]. Recently, all-optical switching has been demonstrated in metallic gratings containing nonlinear optical materials [7,8]. However, as the transmission peak occurs in periodic metal structures, it is very hard to reduce the device to be submicron.

Metal-dielectric-metal (MDM) plasmonic waveguides are important structures in plasmonic devices based on SPPs propagating at metal-dielectric interfaces. They are becoming increasingly popular during the last several years because they not only support modes with deep wavelength scales and high group velocity over a very wide range of frequencies extending from DC to visible [9], but also provide long-range propagation and allow the manipulation and transmission of light at the nanoscale [10]. When they side coupled to nanocavities of different shapes, the formed resonators provide various new functions which are promising for the designing of nanoscale all-optical devices [11–16]. For example, nanoscale channel drop filters have been demonstrated in MDM-based ring and disk resonators [11,12]. Compact filters have been realized in tooth-shaped and stub MDM waveguides [13,14]. Furthermore, all-optical switching has been realized in MDM plasmonic waveguide both directly coupled and side-coupled to square and rectangular cavities based on the absorption [15] and the gain of materials [16]. As is known, the performance of cavity-based nonlinear all-optical devices is critically dependent on the shape of the transmission response. In this paper, we study the transmission response of the nanoscale system consisting of a MDM waveguide and a side coupled nanocavity (SCNC) filled with a Kerr nonlinear medium analytically and numerically. By incorporating an inside-nanocavity (INC) filled with the same nonlinear medium as in the SCNC into the waveguide, the transmission response of the combined structure can be modified to be sharp and asymmetric. As a consequence, the wavelength shift required for the device to be switched from the maximum to the minimum

transmission can be halved in a structure less than 400 nm long. Such an effect may be applied to constructing SPP-based all-optical switching with low power threshold at nanoscale.

## 2. The transmission response from a MDM waveguide side coupled to a nanocavity filled with a nonlinear Kerr medium

We first investigate the transmission response from a MDM waveguide side coupled to a nanocavity filled with a nonlinear Kerr medium. The basic geometry of the structure is shown in the inset of Fig. 1, where  $w_o$  and  $L$  are the width and length of the SCNC,  $d$  denotes the distance between the SCNC and the waveguide.  $w_i$  is the width of the dielectric. Since the width of the MDM waveguide is much smaller than the operating wavelength in our structure, only the excitation of the fundamental waveguide mode is considered. The frequency-dependent complex relative dielectric constant of Ag used in our simulations is characterized by the Drude model with  $(\epsilon_{\infty}, \omega_p, \gamma) = (4.2, 1.346 \times 10^{16} \text{ Hz}, 9.617 \times 10^{13} \text{ Hz})$  [17]. A nonlinear finite-difference time-domain (FDTD) technique [18] with a perfectly matched layer (PML) boundary condition is employed to calculate the transmission spectra. The incident light used to excite SPPs is a TM-polarized (the magnetic field is parallel to the y axis) plane wave. In FDTD simulations, the spatial grid size and temporal step are set as  $\Delta x = 2 \text{ nm}$ ,  $\Delta z = 4 \text{ nm}$  and  $\Delta t = \Delta x/2c$ , respectively. For the nonlinear dielectric medium, we choose its linear refractive index  $n_o = 2$  and nonlinear Kerr coefficient  $n_2 = 5 \times 10^{-3} \text{ } \mu\text{m}^2/\text{W}$  (corresponds to the nonlinear susceptibility  $\chi^{(3)} \sim 1 \times 10^{-8} \text{ esu}$ ) which is obtainable in various materials [17,19]. Then the refractive index of the nonlinear dielectric medium,  $n_d = n_o + n_2 I$ , where  $I$  is the optical intensity in the nonlinear medium. All the transmission of the proposed devices is normalized to the transmission of a straight MDM waveguide with the same length and thus it does not include the propagation loss of the waveguide.

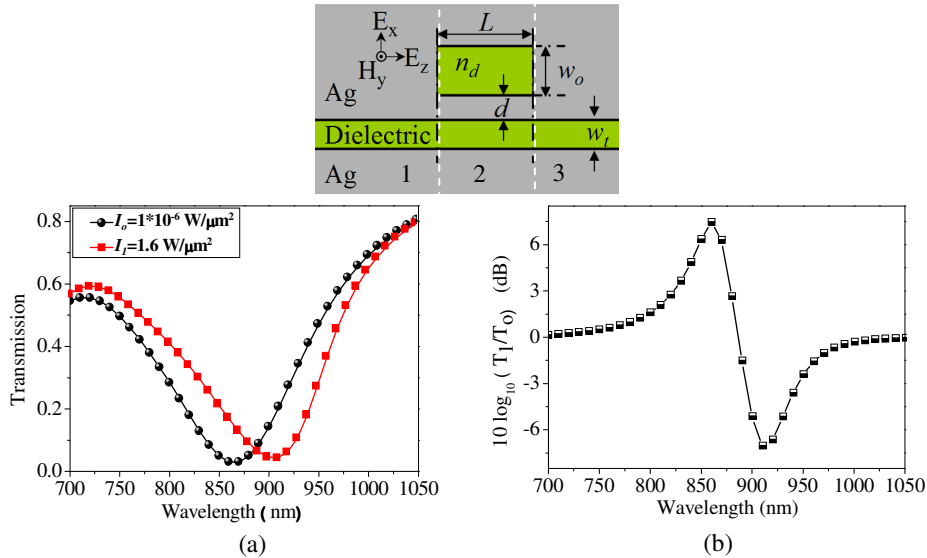


Fig. 1. Inset is the schematic of the structure which is divided into three regions by two white dashed lines. (a) Transmission spectra of the MDM waveguide with the SCNC at two different incident intensities. The geometric parameters of the structure are:  $w_o = 50 \text{ nm}$ ,  $L = 100 \text{ nm}$ ,  $d = 14 \text{ nm}$ ,  $w_i = 30 \text{ nm}$ . (b) The transmission contrast ratio between the two incident light intensities as a function of the incident wavelength.

The nanocavity shown in the inset Fig. 1 behaves as a resonant cavity and supports a resonant mode at a frequency of  $\omega_o$ , which corresponds to a resonant wavelength of  $\lambda_o$ . By

using the temporal coupled-mode theory [16,20], the transmission  $T$  of this system can be described as:

$$T = \frac{(\omega - \omega_o)^2 + (\frac{1}{\tau_o})^2}{(\omega - \omega_o)^2 + (\frac{1}{\tau_o} + \frac{1}{\tau_e})^2} \quad (1)$$

where  $\omega = 2\pi c/\lambda$  is the frequency and  $\omega_o$  the frequency at resonance.  $1/\tau_o$  is the decay rate of the field in the SCNC due to the internal loss, and  $1/\tau_e$  is the decay rate due to the power escape through the waveguide. At the resonant frequency  $\omega_o$ , the incident power is reflected and results in a dip ( $T_{min}$ ) in the transmission spectrum of the structure. Normally, the transmission spectrum exhibits a symmetric Lorentzian line shape. The resonant wavelength  $\lambda_o$  is controlled by the geometry of the SCNC, i.e., the length  $L$  and the width  $w_o$ .  $L$  can be estimated by combining the resonant condition ( $\Delta\phi = m \cdot 2\pi$ ) of forming stable standing waves in the cavity and the phase shift  $\Delta\phi$  of light passing through the SCNC, which is given by,

$$\Delta\phi = \frac{4\pi \text{Re}(n_{eff}) \cdot L}{\lambda_o} \quad (2)$$

where  $n_{eff}$  is the effective refractive index of the SCNC and is related with  $\lambda_o$  and  $w_o$ . Their relationship is determined by [5,21],

$$\tanh(\sqrt{n_{eff}^2 - \epsilon_d} \cdot w_o \pi / \lambda_o) = \frac{-\epsilon_d \sqrt{n_{eff}^2 - \epsilon_m}}{\epsilon_m \sqrt{n_{eff}^2 - \epsilon_d}} \quad (3)$$

The structure parameters of the SCNC are chosen to be  $w_o = 50$  nm and  $L = 100$  nm, thus the resonant wavelength is in the visible wavelength range. From Eq. (2), the resonant wavelength  $\lambda_o$  is obviously related with  $n_{eff}$ , which is dependent on the refractive index  $n_d$  of the SCNC. Therefore,  $\lambda_o$  can be controlled by the light intensity  $I$  through  $n_d = n_o + n_2 I$ . Figure 1(a) exhibits the transmission spectra at two different intensities of the incident light, in which  $d = 14$  nm and  $w_t = 30$  nm. As can be seen, the transmission dip red shifts from 860 nm to 910 nm when  $I$  is increased from  $I_o = 1 \times 10^{-6}$  to  $I_l = 1.6$  W/ $\mu\text{m}^2$ , indicating that the resonant dip can be tuned by the nonlinearity of the Kerr medium in the SCNC. When  $I_o = 1 \times 10^{-6}$  W/ $\mu\text{m}^2$ , the nonlinear response of the Kerr medium is very weak, we can neglect the change of  $n_d$ .  $10\log_{10}(T_l/T_o)$  is defined as the transmission contrast ratio at different wavelengths, where  $T_o$  corresponds to the transmission at  $I_o$  and  $T_l$  at  $I_l$ . As shown in Fig. 1(b), the transmission contrast ratio at the resonant wavelength of 860 nm is 7.4dB. One thing worth noting is that although the shape of the spectra is Lorentzian-like, the two shoulders of the transmission spectra, however, are not symmetric. The reason is that the imaginary part of the propagation constant  $\text{Im}(\beta)$  (corresponding to the loss) is inversely proportional to the wavelength [21]. Therefore, the loss at the shorter wavelength is larger and leads to a lower transmission on the left-hand side of the resonant dip.

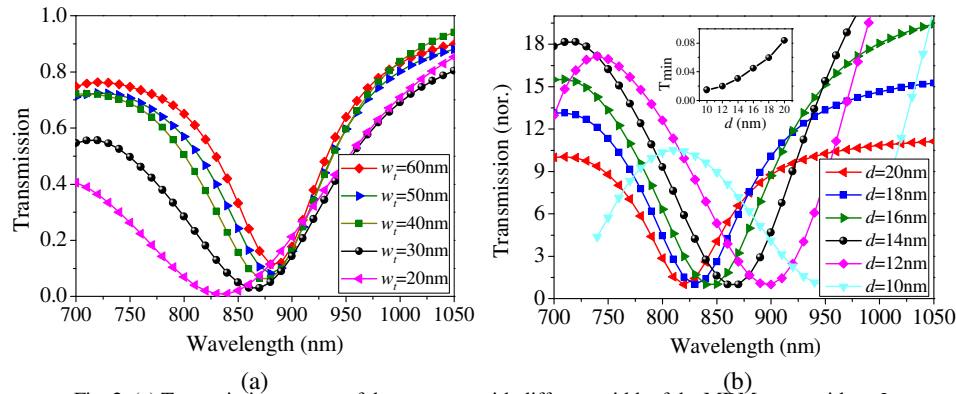


Fig. 2. (a) Transmission spectra of the structure with different width of the MDM waveguide at  $I_o = 1 \times 10^{-6} \text{ W}/\mu\text{m}^2$ . Other geometric parameters of the structure are:  $w_o = 50 \text{ nm}$ ,  $L = 100 \text{ nm}$ ,  $d = 14 \text{ nm}$ . (b) Transmission spectra normalized to  $T_{min}$ . Inset shows  $T_{min}$  as a function of  $d$ .

The response function of the transmission spectrum and the value of the minimum transmission ( $T_{min}$ ) at the resonant wavelength are two important factors to determine the performance of the cavity-based device. The parameters affecting them include  $w_t$  and  $d$ . As shown in Fig. 2(a),  $T_{min}$  decreases with  $w_t$ . The spectral width of the transmission response, however, increases at the same time. Furthermore, as  $\text{Im}(\beta)$  increases with the decrease of the width of the waveguide [21], decreased  $w_t$  will result in a larger propagation loss. Therefore, we choose  $w_t = 30 \text{ nm}$ , which is similar to that in other plasmonic waveguides [4].

The transmission response of the structure is significantly influenced by the distance  $d$ , which controls the coupling strength between the waveguide and the SCNC. Figure 2(b) shows the transmission spectra with different  $d$ , which are normalized to their own minimum to compare the slope of the left-hand edge. As can be seen, with an increase of  $d$ ,  $T_{min}$  increases (shown in the inset) and the width of the resonant spectrum decreases. This can be understood from the following analysis. When  $d$  increases,  $1/\tau_o$  decreases and results in a weaker coupling and thus high quality factor  $Q$  and narrow spectral width of the resonance. As  $1/\tau_o$  is the decay rate of the field in the SCNC due to the internal loss, we can neglect the influence from  $d$ . Therefore, from the coupled-mode theory (Eq. (1)), it can be deduced that  $T_{min}$  increases with  $d$ . Based on these two different trends, i.e.,  $T_{min}$  increases with  $d$  while the resonant spectral width decreases, the slope of the left-hand edge of the spectrum will not change with  $d$  monotonously. As shown in Fig. 2(b), with a decrease of  $d$ , the slope becomes larger at first. When  $d < 14 \text{ nm}$ , the slope starts to decrease. Therefore,  $d = 14 \text{ nm}$  seems the most appropriate distance to obtain a sharp transmission response and a small  $T_{min}$  here. Another phenomenon observed in Fig. 2(b) is that the resonant wavelength blue shifts with an increase of  $d$ . We attribute this to the decrease of the real part of the effective refractive index of the region 2 shown in the inset of Fig. 1.

From Fig. 1(a), a broad resonant width larger than 300 nm width is observed due to losses. The wavelength shift required for the device to be switched from the maximum to the minimum transmission is as large as 150 nm. Furthermore, even with the optimized geometric parameters, the best transmission contrast ratio between the two incident intensities,  $I_o = 1 \times 10^{-6}$  and  $I_l = 1.6 \text{ W}/\mu\text{m}^2$ , is only about 7.4 dB.

### 3. Incorporating an inside-nanocavity containing a Kerr nonlinear medium into the MDM waveguide with the SCNC

Optical bistability can be realized in a MDM plasmonic waveguide directly coupled to an inside-nanocavity (INC) containing a Kerr nonlinear medium, which behaviors as a F-P cavity. The maximum of the transmission contrast ratio at the resonant wavelength, however, is less

than 2 dB [4]. On the other hand, the F-P oscillation can also be utilized as a background to improve the switching performance in photonic crystals [22]. Here, based on the investigation in reference [22], we introduce a F-P nanocavity into the MDM waveguide with the SCNC to modify the shape of the transmission spectrum and explore its potential applications in integrated circuits.

The inset of Fig. 3 plots the combined structure, in which the same nonlinear Kerr dielectric medium as in the SCNC with a length of  $h$  is incorporated into the MDM waveguide and acts a F-P cavity. The presence of the new cavity can perturb the phase of the light directly transmitted through the waveguide. Therefore, a complex interference phenomenon is formed between the SCNC and INC. If we assume the metal is lossless, from the scattering matrix theory, the transmission for the INC without the SCNC is given by [20,22–24],

$$T_{F-P} = \left| \frac{r^2(\lambda) - 1}{\cos \frac{\Delta\phi}{2} - i \sin \frac{\Delta\phi}{2} - r^2(\lambda) (\cos \frac{\Delta\phi}{2} + i \sin \frac{\Delta\phi}{2})} \right|^2 \quad (4)$$

where  $r(\lambda) = [n(\lambda) - 1] / [n(\lambda) + 1]$  is the reflectivity between the air-dielectric interface and  $n(\lambda) = \text{Re}(n_{\text{eff-MAM}}) / \text{Re}(n_{\text{eff-MDM}})$ .  $n_{\text{eff-MAM}} / n_{\text{eff-MDM}}$  is the effective refractive index in the metal-air-metal/metal-dielectric-metal waveguide, respectively. Please note that the dispersion of the reflection is included here.  $\Delta\phi$  is the phase shift when light passes through the INC and can be obtained by Eq. (2) (substituting  $L$  by  $h$ ).

The loss in the SCNC will significantly broaden the width of the resonance and influence the transmission response. Based on the theory in references [20,22–24], an equation to calculate the transmission of the combined structure by combining the transfer matrix of the SCNC and INC with considering the loss in the SCNC and the dispersion of the reflection at the interface forming the INC can be deduced as in the following:

$$T = \left| \frac{[r^2(\lambda) - 1](\omega - \omega_0 + i \frac{1}{\tau_o})}{(\omega - \omega_0 + i \frac{1}{\tau_e} + i \frac{1}{\tau_o}) (\cos \frac{\Delta\phi}{2} - i \sin \frac{\Delta\phi}{2}) - (\omega - \omega_0 - i \frac{1}{\tau_e} + i \frac{1}{\tau_o}) [r^2(\lambda) \cdot \cos \frac{\Delta\phi}{2} + i r^2(\lambda) \cdot \sin \frac{\Delta\phi}{2}] - 2ir(\lambda) \cdot \frac{1}{\tau_e}} \right|^2 \quad (5)$$

where  $1/\tau_o$  and  $1/\tau_e$  have the same meanings as in Eq. (1). We neglect the loss in the INC here as it mainly influences the background of the transmission response of the combined structure. Normally, if the metal is assumed to be lossless, the spectral width at resonant is around 10 nm (in the near infrared wavelength range) [16]. If we consider the loss in the SCNC (without losing the generality, we assume  $1/\tau_e = 1.4 \times 10^{14}$  Hz and  $1/\tau_o = 0.3 \times 10^{14}$  Hz), the spectral width of the transmission responses determined by Eq. (5) are broaden to be larger than 300nm, as shown in Fig. 3(a). The response function of the transmission spectrum from the INC determined by Eq. (4) is also displayed in Fig. 3(a). As observed, the shape of the resonant feature depends critically on the relative position of the resonant wavelength of the system with respect to the F-P oscillation. When the resonant wavelength ( $\lambda_o = 1050\text{nm}$ ) coincides with a maximum of the F-P oscillation, the transmission response exhibits a Lorentzian line shape. As it moves to the shorter/longer wavelength, the symmetry of the transmission spectrum is broken and its left/right-hand edge becomes sharp. For example, when the resonant wavelength moves from 1050 nm to 920 nm, the wavelength shift required to switch the system from  $T_{\text{max}}$  to  $T_{\text{min}}$  is reduced from 120 nm to 50 nm on the left-hand side of the resonant dip. To verify the analytic results, we simulate the transmission response of the system by the FDTD technique. Based on the relationship in Eq. (2) and Eq. (3), we adjust the position of the resonant dip  $\lambda_o$  by changing  $w_o$ . As can be seen in Fig. 3(b), the numerical experiment results are basically consistent with

those calculated by the analytic theory, suggesting that our analytic model is reasonable. The lower transmission in the FDTD modeling results is due to the loss in the INC. The point we emphasize here is that even with the loss in the SCNC and the dispersion of the reflection, the transmission response of the system can be modified to be sharp and asymmetric by the background F-P oscillation without gain materials.

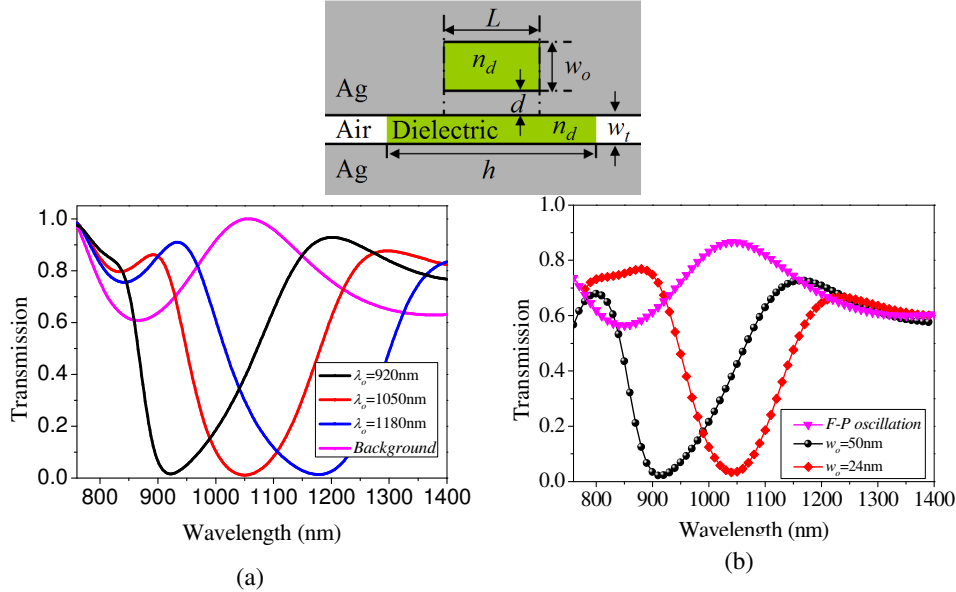


Fig. 3. Top inset is the schematic of the combined structure. (a) Theoretical transmission spectra of the device calculated from Eq. (5) (black, red and blue lines). The magenta line represents the response from the background F-P oscillation [from Eq. (4)] without the SCNC. (b) Transmission spectra with two different  $w_o$  obtained by FDTD simulation at incident intensity:  $I_o = 1 \times 10^{-6} \text{ W}/\mu\text{m}^2$ . The geometric parameters of the structure are:  $h = 320 \text{ nm}$ ,  $w_l = 30 \text{ nm}$ ,  $d = 14 \text{ nm}$ .

The decrease of the bandwidth to switch the system from  $T_{max}$  to  $T_{min}$  in cavity-based systems is significant for reducing the wavelength shift required for realizing nonlinear all-optical devices such as switches and modulators. For instance, when the intensity is tuned from  $I_o = 1 \times 10^{-6} \text{ W}/\mu\text{m}^2$  to  $I_l = 1.6 \text{ W}/\mu\text{m}^2$ , the resonant wavelength shifts from 860 nm to 940 nm, which is almost equal to the bandwidth of the left-hand side of the resonant function and the system is switched from  $T_{min}$  (at  $I_o$ ) to  $T_{max}$  (at  $I_l$ ), as shown in Fig. 4(a). In addition, Fig. 4(b) exhibits that the transmission contrast ratio at the resonant wavelength reaches 14 dB and is significantly improved compared to that (7.4 dB) in the system with the SCNC only.

The steady magnetic field distributions of the device at two incident light intensities are shown in Fig. 4(c). As seen, when the intensity of the incident light  $I_o = 1 \times 10^{-6} \text{ W}/\mu\text{m}^2$ , the incident optical mode at the resonant wavelength of 860 nm is almost completely reflected. In contrast, when  $I_l = 1.6 \text{ W}/\mu\text{m}^2$ , the transmitted light in the right hand-side of the device is clearly visible. This may be potentially applied as a nanoscale all-optical switch in optical integrated circuits.

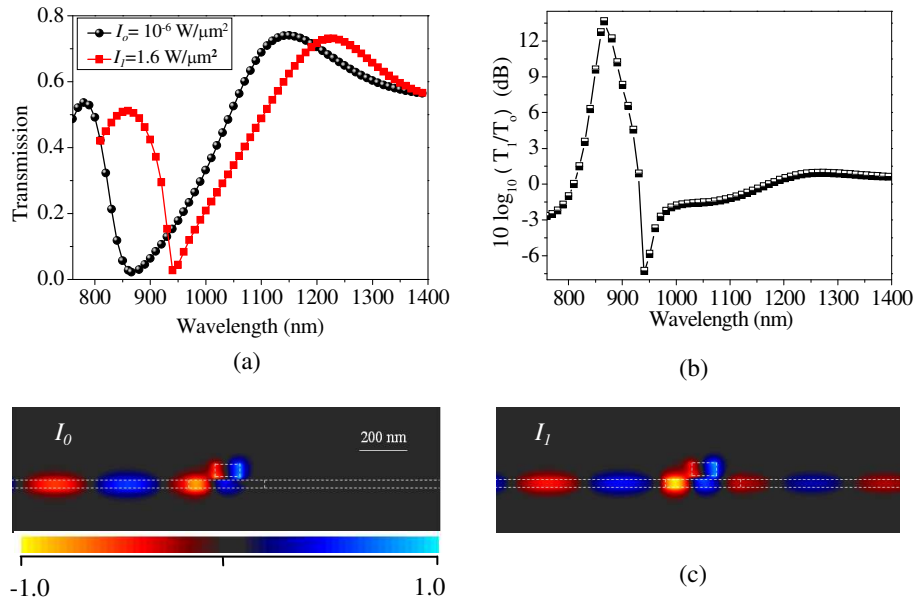


Fig. 4. (a) Transmission spectra at incident intensities:  $I_o = 1 \times 10^{-6} \text{ W}/\mu\text{m}^2$  (black),  $I_t = 1.6 \text{ W}/\mu\text{m}^2$  (red). The geometric parameters of the structure are:  $h = 320 \text{ nm}$ ,  $w_t = 30 \text{ nm}$ ,  $d = 14 \text{ nm}$ . (b) Transmission contrast ratio between the two different incident light intensities. (c) Spatial evolutions of the magnetic field profile (at  $\lambda_o = 860 \text{ nm}$ ) at two different incident intensities. The signal light is incident from the left-hand side.

#### 4. Conclusions

To summarize, we have analytically and numerically investigated the transmission response in metal-dielectric-metal (MDM) plasmonic waveguides with a side coupled nanocavity (SCNC) based on the excitation of SPPs. The transmission dip can be tuned by the incident light intensity through the Kerr nonlinear phenomenon in the nanocavity. A background oscillation formed by incorporating a finite length of the same Kerr nonlinear media into the MDM waveguide can tune the shape of the transmission response line to be sharp and asymmetric. As a consequence, the wavelength shift required for the device to be switched from the maximum to the minimum transmission can be halved in a structure less than 400 nm long. Such an effect may be potentially applied to constructing SPP-based all-optical switching with low power threshold at nanoscale.

#### Acknowledgments

The authors acknowledge the financial support from the National Natural Science Foundation of China (Grant Nos. 10774050 and 10674051) and the Program for Innovative Research Team of the Higher Education in Guangdong (Grant No. 06CXTD005). The author Mr. Zhong Zhijian gratefully acknowledges Dr. Min Changjun in Louisiana State University for useful discussions.